

**Change of AOT and
aerosol DRE to RH**

H. Bian et al.

Sensitivity of aerosol optical thickness and aerosol direct radiative effect to relative humidity

H. Bian^{1,2}, M. Chin², J. Rodriguez², H. Yu^{1,2}, J. E. Penner³, and S. Strahan^{1,2}

¹Goddard Earth Sciences and Technology Center, University of Maryland, Baltimore County, Baltimore, Maryland, USA

²Atmospheric Chemistry and Dynamics Branch, NASA Goddard Space Flight Center, Greenbelt, Maryland, USA

³Department of Atmospheric, Oceanic and Space Sciences, University of Michigan, Ann Arbor, Michigan, USA

Received: 20 February 2008 – Accepted: 17 June 2008 – Published: 11 July 2008

Correspondence to: H. Bian (huisheng.bian@nasa.gov)

Published by Copernicus Publications on behalf of the European Geosciences Union.

Title Page

Abstract

Introduction

Conclusions

References

Tables

Figures

◀

▶

◀

▶

Back

Close

Full Screen / Esc

Printer-friendly Version

Interactive Discussion



Abstract

We present a sensitivity study on the effects of spatial and temporal resolution of atmospheric relative humidity (RH) on calculated aerosol optical thickness (AOT) and the aerosol direct radiative effects (DRE) in a global model. Using the same aerosol fields simulated in the Global Modeling Initiative (GMI) model, we find that, on a global average, the calculated AOT from RH in 1° latitude by 1.25° longitude spatial resolution is 11% higher than that in 2° by 2.5° resolution, and the corresponding DRE at the top of the atmosphere is 8–9% higher for total aerosols and 15% higher for only anthropogenic aerosols in the finer spatial resolution case. The difference is largest over surface escarpment regions (e.g. >200% over the Andes Mountains) where RH varies substantially with surface terrain. The largest zonal mean AOT difference occurs at $50\text{--}60^\circ\text{N}$ (16–21%), where AOT is also relatively larger. A similar increase is also found when the time resolution of RH is increased. This increase of AOT and DRE with the increase of model resolution is due to the highly non-linear relationship between RH and the aerosol mass extinction efficiency (MEE) at high RH (>80%). Our study suggests that caution should be taken in a multi-model comparison (e.g. AeroCom) since the comparison usually deals with results coming from different spatial/temporal resolutions.

1 Introduction

Relative humidity (RH) can significantly influence ambient aerosol optical thickness (AOT) and, therefore, aerosol direct radiative forcing (Kinne et al., 2003; Malm et al., 2005; Pahlow et al., 2006). For example, the AOT at 550 nm measured during ACE-Asia was tripled when the RH increased from 50% to 95% (Yoon and Kim, 2006). Accounting for the impact of RH on AOT in CTM simulations requires not only good performance of the underlying GCM in simulating the moisture field, but also a practical consideration of spatial and temporal resolution of the RH field because of the high

Change of AOT and aerosol DRE to RH

H. Bian et al.

Title Page

Abstract

Introduction

Conclusions

References

Tables

Figures

◀

▶

◀

▶

Back

Close

Full Screen / Esc

Printer-friendly Version

Interactive Discussion



heterogeneity of RH in both space and time. This RH representative issue is directly relevant to the work of AeroCom, a model intercomparison effort to assess aerosol properties and their atmospheric influence, which often involves models with different spatial resolutions (Kinne et al., 2006; Schulz et al., 2006; Textor et al., 2006). For example, the horizontal resolutions range from $1.1^\circ(\text{latitude}) \times 1.1^\circ(\text{longitude})$ to $10^\circ \times 22.5^\circ$ in 20 models involved in the assessment of multi-model optical properties by Kinne et al. (2006).

The non-linear relationship of RH and aerosol mass extinction efficiency (MEE) results in the issue of RH representativeness in AOT calculation. MEE multiplied with aerosol dry mass determines AOT. Figure 1 shows the change of MEE of sea salt particles (left) and internally mixed fossil fuel particles (right) as a function of RH. The figure indicates that the change of aerosol MEE with RH is highly non-linear especially at $\text{RH} > 80\%$. In other words, a small uncertainty in RH under ambient conditions will translate into a very large uncertainty in MEE. Due to this non-linear relationship, the sub-grid RH variation will inevitably yield an AOT difference among AOTs which are calculated by different spatial (or temporal) averaged RHs even though the RHs originate from the same GCM.

The objective of this paper is to investigate the potential AOT changes induced solely from the different RH spatial and temporal resolutions in global models. This study helps us to estimate the extent to which the AOT diversities in the AeroCom models may be caused just by different model resolutions. We will address this issue from a single global model framework and for all aerosol components simulated in the model. Specifically, we will answer:

1. What is the AOT variation in terms of RH representation for two typical spatial resolutions (i.e. $1^\circ(\text{latitude}) \times 1.25^\circ(\text{longitude})$ vs. $2^\circ \times 2.5^\circ$) and for two typical time intervals (i.e. 3 h vs. 6 h) over which RH is averaged?
2. Where and when is the AOT most sensitive to the different representations of RH?

Change of AOT and aerosol DRE to RH

H. Bian et al.

[Title Page](#)[Abstract](#)[Introduction](#)[Conclusions](#)[References](#)[Tables](#)[Figures](#)[I◀](#)[▶I](#)[◀](#)[▶](#)[Back](#)[Close](#)[Full Screen / Esc](#)[Printer-friendly Version](#)[Interactive Discussion](#)

Change of AOT and aerosol DRE to RH

H. Bian et al.

[Title Page](#)[Abstract](#)[Introduction](#)[Conclusions](#)[References](#)[Tables](#)[Figures](#)[I◀](#)[▶I](#)[◀](#)[▶](#)[Back](#)[Close](#)[Full Screen / Esc](#)[Printer-friendly Version](#)[Interactive Discussion](#)

The examined RH resolutions (Table 1) are the most common resolutions used in the current models. For example, 13 out of 20 models evaluated by Kinne et al. (2006) have a horizontal resolution close to $2^\circ \times 2.5^\circ$. In addition, we will use a radiative transfer model to examine the variations of aerosol DRE at the top of atmospheric (TOA) due to the AOT differences resulting from different resolutions to give an overall estimation of the effect on climate.

Our study extends a previous idealized study on the effects of sub-grid variations of RH on the direct radiative forcing (DRF) of sulfate aerosol using a limited-area-model (Haywood et al., 1997). The study found that the estimated DRF (the difference in DRE simulated with and without sulfate aerosol) using a low resolution (160 km by 160 km) was approximately 73% and 60% lower than that using a high resolution (2 km by 2 km) for clear sky and cloudy sky, respectively.

We first describe in Sect. 2 the models used in this study and the three sensitivity experiments. We then show the results of model AOT calculated at different spatial and temporal resolutions and discuss reasons for those differences in Sect. 3.1 to 3.4. The corresponding changes of DRE are shown in Sect. 3.5. Finally the conclusions and implications of the study are given in Sect. 4.

2 Model description and experiment design

2.1 GMI aerosol module

The Global Modeling Initiative (GMI) model is designed to maintain a modular 3-D CTM that can be used to assess the impact of various natural and anthropogenic perturbations on atmospheric composition and chemistry (e.g., Strahan and Douglass et al., 2004; Strahan et al., 2006, 2007; Considine et al., 2004; Douglass et al., 2004, 2006; Liu et al., 2007). GMI can be driven by several different meteorological fields (Liu et al., 2007). In this study, we use the assimilated meteorological fields from NASA's Goddard Earth Observation System Version 4 (GEOS-4) data assimilation system (DAS)

(Bloom et al., 2005). The original GEOS-4 DAS data have a spatial resolution of 1° latitude, 1.25° longitude, and 55 vertical layers with a top lid at 0.01 mb, but they are usually degraded to 2° latitude, 2.5° longitude, and 42 vertical layers (reduced layers in stratosphere) for GMI simulations. The GEOS-4 DAS meteorological fields are archived once every 3 h.

The general physical and chemical processes in GMI for aerosols have been described by Liu et al. (2007). The model simulates aerosol mass distribution for sulfate, black carbon, organic carbon, dust, and sea salt. Instead of using the prescribed emissions in Liu et al. (2007), the dust and sea-salt emissions are calculated in GMI with the emission algorithms similar to those in the GOCART model (Ginoux et al., 2001; Chin et al., 2002, 2004). Briefly, dust emission rates of eight size groups (0.1–10 μm) are calculated as a function of surface topographic depression, surface type, 10 m wind speed, and surface wetness (Ginoux et al., 2001), and sea salt emissions for 4 size groups (0.1–10 μm) are calculated as a function of surface wind speed (Monahan et al., 1986; Gong et al., 1997, 2003). For all aerosol type and size groups, lognormal distributions are assumed.

Three aerosol optical properties (AOT, single scattering albedo (ω), and asymmetry factor (g)) were calculated for the AOT analyses and for the radiative transfer simulation. The AOT is calculated using the aerosol mass combined with aerosol MEE. Aerosols originating from fossil fuel are assumed to be internally mixed, as are aerosols from biomass burning. All other aerosols are externally mixed. MEEs are calculated by Mie scattering theory for each of the particle types, i.e. each of the eight dust bin sizes, fine mode and coarse mode of sea salt, internally mixed fossil fuel particle, internally mixed biomass burning particle, natural sulfate, and natural OC, by given the corresponding size distribution and complex refractive index of each particle type. Aerosol MEEs (as are AOT, ω , and g) are RH dependent except dust. The three properties are also wavelength dependent in order to account for the effect of the whole shortwave spectrum for DRE. However, only AOT (550 nm) is used in the AOT-RH analyses. The refractive index of internally mixed aerosols is determined by volume weighted refrac-

Change of AOT and aerosol DRE to RH

H. Bian et al.

[Title Page](#)[Abstract](#)[Introduction](#)[Conclusions](#)[References](#)[Tables](#)[Figures](#)[◀](#)[▶](#)[◀](#)[▶](#)[Back](#)[Close](#)[Full Screen / Esc](#)[Printer-friendly Version](#)[Interactive Discussion](#)

tive indices of the individual aerosols. The size distribution and the hygroscopic growth factors for internally mixed fossil fuel and biomass burning particles, as well as for natural sulfate and organic matter, are described in Liu et al. (2007). The optical properties for dust and sea-salt are from Chin et al. (2002). The calculated aerosol MEE is tabulated as a function of aerosol types, relative humidity, size bins, and the mass fraction of BC (for fossil fuel and biomass burning aerosols).

2.2 Radiative transfer model

The aerosol direct effect on solar radiation is calculated with the Goddard Space Flight Center radiative transfer model (Chou and Suarez, 1999; Chin et al., 2001; Weaver et al., 2001). This model accounts for absorption by O₃, CO₂, O₂, H₂O, and aerosols, and accounts for scattering by clouds, aerosols, and gases. The solar spectrum (0.2 to 10 μm) is divided into eight bands in the UV and visible range and three bands in the near infrared.

Three aerosol radiative properties described in Sect. 2.1 determine the aerosol radiative effect. In addition to the aerosol information, the radiative transfer code requires fields of temperature, specific humidity, cloud optical thickness, cloud fraction, and surface albedoes. These fields are supplied by the GEOS-4 DAS meteorological fields.

2.3 Experimental setup

We performed three experiments (Table 1) to investigate the differences in model calculated AOT and aerosol DRE resulting from the use of different spatial and temporal resolutions of the RH field. In all three experiments, the RH was obtained from the GEOS-4 DAS, and the GMI simulated aerosol mass was unchanged in order to highlight the AOT change solely due to the RH resolution change.

We first calculated AOT using the RH at the typical GMI model resolution, which is 3 h in time and 2° latitude by 2.5° longitude with 42 vertical layers in space. Recall that in this case, the RH field had been degraded from the original GEOS-4 DAS 1°x1.25°

Title Page

Abstract

Introduction

Conclusions

References

Tables

Figures

◀

▶

◀

▶

Back

Close

Full Screen / Esc

Printer-friendly Version

Interactive Discussion



resolution. We denote this calculation as the base case (BASE).

We then conducted two sensitivity studies, each differs from BASE in horizontal or temporal resolution: in the first one, the horizontal resolution of the RH was increased from 2° latitude \times 2.5° longitude in BASE to the original GEOS-4 DAS resolution of $1^\circ \times 1.25^\circ$ (a factor of 4 increase of spatial resolution), while in the second case, the RH time resolution was decreased from the 3-h average in BASE to a 6-h average (a factor of 2 increase of temporal resolution).

All experiments are run for one and half year (1 July 2000–31 December 2001) with the first half year as a spin up time.

3 Results

In this section, we first examine the AOT simulation in the base case (Figs. 2 and 3), and then summarize the relationship between AOT and RH in terms of the change in the RH spatial and temporal resolution. The variations in AOT caused by the different RH resolutions are shown in Figs. 4–7.

3.1 The AOT simulation in the base case

The base case AOT from the GMI model is compared with satellite measurements from MODIS and MISR in Fig. 2 for April 2001. Overall, the GMI captures the main features of the observed AOT. For example, both model and satellite data show very high AOTs over Southeast Asia and east Asia. This is because April is the month with high biomass burning emission over Southeast Asia and with high dust events over east Asia along Taklimakan, Mongolia, and Gobi regions. The other high AOTs are evident over polluted land areas such as Western Europe and Eastern North America and over the deserts such as in western Africa, as well as downwind from these regions. The lowest AOT occurs typically during SH tropical region. Nevertheless, the modeled AOT is generally lower than satellite observations over most remote oceans.

Title Page

Abstract

Introduction

Conclusions

References

Tables

Figures

◀

▶

◀

▶

Back

Close

Full Screen / Esc

Printer-friendly Version

Interactive Discussion



Change of AOT and aerosol DRE to RH

H. Bian et al.

[Title Page](#)[Abstract](#)[Introduction](#)[Conclusions](#)[References](#)[Tables](#)[Figures](#)[I◀](#)[▶I](#)[◀](#)[▶](#)[Back](#)[Close](#)[Full Screen / Esc](#)[Printer-friendly Version](#)[Interactive Discussion](#)

The base case AOT from the GMI model is also compared with available AERONET measurements in April 2001 in Fig. 3. The correlation of the two datasets is quite high ($R=0.81$). The relative bias (B), which is defined as a ratio of the sum of model AOTs versus the sum of measured AOTs over the AERONET stations, indicates that the overall model AOT is slightly lower than that of the measurement ($B=0.79$). Considering the lower model oceanic AOT than that of satellites as discussed in the above model-satellite comparison, the calculated B might be reduced if more ocean station measurements were involved.

As we will discuss in the next section, the model resolution might contribute to the AOT underestimation in our base case simulation.

3.2 Effect of the change RH spatial resolution on AOT

Monthly mean AOT differences associated with the change of RH horizontal resolution for April 2001 are shown in Fig. 4. The upper panel of the figure shows the absolute difference [$AOT(CTR_H) - AOT(BASE)$] and the lower panel shows the relative difference [$(AOT(CTR_H) - AOT(BASE)) / AOT(BASE)$]. The figure shows that regional AOT is sensitive to the choice of the two prescribed RH horizontal resolutions (Table 1). The highest AOT difference generally occurs over regions with high hygroscopic aerosol loading, such as NH middle latitudes, or in regions with sharp RH spatial gradients, such as land/ocean boundaries and surface escarpments. The AOT change is particularly sensitive to the last case; for example, the relative difference is typically more than 200% over the Andes Mountains.

A feature revealed in the figure is that the AOT is always enhanced when the RH horizontal resolution is increased. The numerical reason behind this is the non-linear relationship between AOT and RH (Fig. 1). As such, the method of calculating AOT using sub-grid RH first and then averaging will always yield a higher value than that from the method of averaging RH first (obtaining RH at low resolution) and then calculating AOT.

To further investigate where the AOT is most sensitive to the change in the RH spa-

tial resolution, we averaged the AOT differences over every 10° of latitude using the entire year (2001) simulation. The corresponding annual averaged zonal mean AOT relative and absolute changes are shown in Fig. 5. A large AOT difference (~13–21%) occurs over the middle latitudes in the NH, similar to what is shown in Fig. 4. The maximum change occurs at 50–60°N with a value of 0.03, which is equivalent to 18% of the local mean AOT. There is a weak peak of absolute AOT change over the Southern Hemisphere (SH) storm track (40–65°S) which is dominated by high hygroscopic sea salt particles. The months when zonal mean AOT change reaches its maximum or minimum values during the year are also calculated. However, no apparent time pattern can be identified. Also shown in Fig. 5 are the differences over three major pollution regions: eastern US (A), Western Europe (E), and eastern China (C). The large AOT change in these regions reflects the high hygroscopic properties of the pollution aerosols which are dominated by sulfate.

An analysis similar to Fig. 3 (BASE) is conducted using the model AOT at the high horizontal resolution (CTRH). The correlation coefficient of CTRH remains the same as that of BASE, but the relative bias (B) of AOTs between the model and AERONET is increased from 0.79 in the BASE case to 0.86 in the CTRH case. Thus, increasing resolution does improve the model performance in this study.

3.3 Effect of the change in RH temporal resolution on AOT

The monthly AOT difference for April 2001 derived from simulations with RH averaged over 3-h and 6-h time resolutions is shown in Fig. 6 with absolute difference [AOT(BASE)-AOT(CTRT)] in the upper panel and relative difference [(AOT(BASE)-AOT(CTRT))/AOT(CTRT)] in the lower panel. Similar to Fig. 4, AOT increases with the increase of RH resolution. This increase is largest over the NH mid-latitudes and the SH storm track. There is no significant AOT change in Fig. 6 over high mountainous regions. Figure 6 also elucidates that the regions dominated by dust usually have the smallest AOT change.

Figure 7 shows that the zonal averaged differences in AOT change with the RH

Change of AOT and aerosol DRE to RH

H. Bian et al.

Title Page

Abstract

Introduction

Conclusions

References

Tables

Figures

◀

▶

◀

▶

Back

Close

Full Screen / Esc

Printer-friendly Version

Interactive Discussion



5 resolution, binned in 10° latitudes for year 2001. The magnitude of the AOT change attributed to the prescribed RH temporal resolution (Fig. 7) is less than half of that attributed to RH spatial resolution (Fig. 5), however, the former AOT change may be not that trivial considering that there is just a factor of 2 in temporal resolution change but
10 a factor of 4 in spatial resolution change. The maximum zonal mean AOT relative and absolute changes occur over the middle latitudes in both hemispheres, with equivalent magnitudes of 0.012 (absolute) and 6–8% (relative) variations. Unlike the case with varying RH spatial resolutions, the maximum AOT change due to RH temporal resolution shows a seasonal pattern. In the SH, the maximum difference occurs during late
15 austral winter and early austral spring, while in the NH, it occurs during the late boreal fall and ends in spring. The three regions with high industrial pollution again show high AOT changes, similar to Fig. 4.

3.4 Factors controlling in the variation of AOT with RH resolution

15 To gain insight to why the choice of the RH resolution is important for the AOT simulation shown in Figs. 4–7. Figure 8 upper panel shows the monthly average RH field for April 2001 at 930 mb. Generally, the RH is higher than 80% over most ocean regions where the AOT change with RH resolution tends to be largest when there is high loading of hydrated aerosol particles. Over land area, however, RH shows ranges from less than 20% over northwest Africa (Sahara desert) to more than 90% over northern
20 South America, with the majority of land area lower than 80%. Particularly over desert regions, such as the Sahara desert in Africa, the Indian desert along the Indus valley, the Taklimakan desert in East Asia, Lake Eyre basin in northwest Australia, the Salton Sea in southern California, and Altiplano and Patagonia in the Andes (Ginoux et al., 2001), the RH is typically lower than 40%. In these regions, there is little change of
25 AOT with the change of RH resolution. The primary reason is that these regimes are dominated by hydrophobic particles of dust. In addition, the extremely low RH over these regions lead to the insensitivity of MEE to the change of RH (Fig. 1) even for the inflow hydrated aerosols.

Change of AOT and aerosol DRE to RH

H. Bian et al.

Title Page

Abstract

Introduction

Conclusions

References

Tables

Figures

◀

▶

◀

▶

Back

Close

Full Screen / Esc

Printer-friendly Version

Interactive Discussion



Change of AOT and aerosol DRE to RH

H. Bian et al.

[Title Page](#)[Abstract](#)[Introduction](#)[Conclusions](#)[References](#)[Tables](#)[Figures](#)[◀](#)[▶](#)[◀](#)[▶](#)[Back](#)[Close](#)[Full Screen / Esc](#)[Printer-friendly Version](#)[Interactive Discussion](#)

In addition to the RH magnitude and the atmospheric aerosol composition, the variation of RH in spatial and temporal distributions is also a key factor in determining where and when a large AOT change occurs. A large AOT change occurs when there are a large value of RH and a large RH spatial/temporal variation. An overall explanation of how these two factors in determining the AOT changes is given in Fig. 9. The 3-h RH curves on the figure depict the RH temporal variation during April 2001 over 4 selected sites, two over land and two over ocean (see white circles on Fig. 8 upper panel). Both land sites, site A in East Asia (110°E, 28°N) and site E in Western Europe (30°E, 56°N), have high pollutant aerosols and have comparable absolute AOT differences, 0.020 for site A and 0.018 for site E (Fig. 6). Nevertheless, the RH characteristics at the two sites are apparently different. The monthly mean RH for site A is 95.5% which is much higher than that for site E 69.9% (Fig. 9 upper panel and Fig. 8 upper panel), while the RH daily variation is much smaller at site A than at site E (Fig. 9). These opposite effects compensate each other; ultimately their overall impact on the simulated AOT at the two sites is very similar. On the other hand, the two ocean sites have a substantial difference in absolute AOT change, 0.001 for a site residing in the Indian Ocean in SH middle latitudes (I:90°E, 30°S) and 0.01 for a site within the SH storm track (S:30°E, 60°S) (Fig. 6 upper panel). Figure 9 (lower panel) indicates that the two sites have a similar monthly mean RH, 86.6% for site I and 87.6% for site S. However, the two sites differ in the RH temporal variation, which results in a large discrepancy of AOT change between the two sites.

Many factors, involved in weather system, can impact the variation of the RH field directly or indirectly; among them, surface topography is particularly important in certain regions. The effect of topography on the spatial variation of RH, and its translation to AOT change by adopting different RH resolutions, is elucidated in Figs. 8 (lower panel) and 4. The vertical distribution of RH at a slice at 20°S for April 2001 shows a break in the RH over the Andes Mountains around longitude 60°–70°W. Accordingly, the maximum relative AOT change over the mountain area can be more than 200% (Fig. 4 lower panel). Such regions require a better RH representation regardless of

how good of the underlying GCM calculation. Of course, such regions are usually the most difficult regions for determining the RH in an underlying GCM, which is, however, not the focus of this study.

3.5 Effect of the change in RH on the aerosol DRE

To understand the importance of the sub-grid scale change in RH for climate studies, we analyzed here the change of aerosol TOA DRE (Wm^{-2}) due to the different RH resolutions. To do so, we applied the radiation code described in Sect. 2.2 to calculate DREs with and without aerosols respectively. The difference between them is aerosol DRE. We repeated such calculations with the AOT, ω , and g obtained from different spatial and temporal resolutions of RH, as described in Sect. 3.1 to 3.3.

The aerosol TOA DREs of the three experiments are given in Table 2. The data were averaged over ocean, land, and global areas for clear sky and whole sky, respectively. The percentage changes of the aerosol DREs between the controlled and base cases are listed in the table too.

In the base case, clear sky aerosol DRE at TOA over ocean regions is -4.4 W/m^2 , comparable to other estimates. For example, Yu et al. (2006) estimated this value to be -4.1 W/m^2 with GOCART model simulation, -5.9 W/m^2 using the data of Moderate resolution Imaging Spectroradiometer (MODIS), and -5.5 W/m^2 with the data combining Clouds and the Earth's Energy System (CERES) radiances with aerosol properties from the MODIS level 2 daily aerosol retrievals at a resolution of 10km. Zhang et al. (2005) estimated this value to be $-5.3 \pm 1.7 \text{ W/m}^2$ using aerosol and cloud data from CERES and MODIS. Over land regions, however, the aerosol clear sky DRE (-8.4 W/m^2) given by the base case study is much higher than the estimates of Pata-dia et al. (2008) ($-5.1 \pm 1.14 \text{ W/m}^2$) and Yu et al. (2006) ($-4.5 \pm 0.4 \text{ W/m}^2$). Analysis of speciation contribution indicated that about half of the land aerosol DRE (-3.9 W/m^2) comes from the dust particles.

The clear sky TOA DRE is enhanced by 8.9% (ocean), 8.0% (land), and 8.4% (global) when the RH horizontal resolution is increased from $2^\circ \times 2.5^\circ$ to $1^\circ \times 1.25^\circ$.

Title Page

Abstract

Introduction

Conclusions

References

Tables

Figures

◀

▶

◀

▶

Back

Close

Full Screen / Esc

Printer-friendly Version

Interactive Discussion



Change of AOT and aerosol DRE to RH

H. Bian et al.

A slightly higher variation over ocean areas comes from the fact that the ocean aerosol DRE is dominated by the hydrophilic species of sea salt (1/3 of total) and anthropogenic particles (1/3 of total) with dust (~8%) and the other nature aerosols contributing to the rest, while the land DRE is dominated by both anthropogenic particles (1/3 of total) and hydrophobic dust particles (~1/2 of total) with a small fraction from sea salt (~3%) and other nature aerosols. The TOA aerosol DRE is reduced by 20–25% from the clear sky condition to the whole sky, however, the changes of aerosol TOA DRE due to the changes of RH horizontal resolutions in both conditions are comparable. The change of aerosol TOA DRE due to the change of RH temporal resolution is only about 1/3 of that due to the change of RH horizontal resolution in both conditions (Again, the magnitude of RH temporal resolution change is only half of that in special resolution change). Regionally, the change in the aerosol TOA DRE is higher over the middle latitudes of both hemispheres, similar to the pattern of the AOT change.

Considering anthropogenic aerosols alone, the whole sky TOA DREs would be –2.48 (land), –0.95 (ocean), and –1.41 (global) for the base case study and they are enhanced to be –3.33/–1.26/–1.86 respectively in the clear sky condition. The changes of the TOA DREs due to different spatial resolutions are 16.9%/13.7%/15.1% for the whole sky condition and 15.6%/12.7%/14.9% for the clear sky condition. These changes are larger than those contributed from all aerosols even over oceans. This behavior can be confirmed from the Fig. 1 which shows that the sensitivity of MEE to RH is much higher for anthropogenic aerosols than for sea-salt aerosols.

The change of aerosol TOA DRE due to the change of the RH resolutions is not large considering that it has a wide range of aerosol DRE estimates from literature based on measurements and model simulations. Nevertheless, the change is systematic: the higher the resolution, the higher the TOA DRE.

[Title Page](#)[Abstract](#)[Introduction](#)[Conclusions](#)[References](#)[Tables](#)[Figures](#)[I◀](#)[▶I](#)[◀](#)[▶](#)[Back](#)[Close](#)[Full Screen / Esc](#)[Printer-friendly Version](#)[Interactive Discussion](#)

4 Conclusions

We investigated the impacts of using RHs representing different spatial and temporal resolutions on AOT and aerosol TOA DRE simulations. One firm conclusion is that AOT and TOA DRE always increase with an increase in the RH resolution. On a global basis, the AOT increases by 11% with the higher spatial resolution and 4% with the higher temporal resolution (note that the magnitude of spatial resolution change is twice of that of temporal resolution change). Correspondingly, DRE at the TOA increases by 9% and 3% for a use of the higher spatial and temporal resolution respectively. Accounting for anthropogenic aerosols alone for both clear and whole skies increases the TOA DRE of the finer spatial resolution even higher by 15% because the sensitivity of MEE to RH is much higher for anthropogenic aerosols than for sea-salt aerosols. On a regional scale, the influence of the higher spatial resolution of RH becomes much stronger. The AOT usually increases by more than 20% over Western Europe and Eastern North America (note that the AOT itself is also higher over these regions) and could increase by more than a factor of 2 over the Andes Mountains. Overall, the AOT change is larger in middle latitudes than in tropical regions, largely because of the larger contribution of hydrophobic dust in tropical regions.

Two features of the RH field, its magnitude and variation, are key factors in determining where and when AOT is most sensitive to RH. Over low RH regions, such as deserts, AOT is insensitive to the choice of RH resolution due to both the aerosol composition (dust dominated) and aerosol optical property (small MEE change even for hygroscopic aerosols) in such regions. Over high RH regions, such as over most ocean areas, Europe, and the east coasts of continents, the importance of relative humidity (RH) on aerosol optical thickness (AOT) is substantially amplified because of hygroscopicity of aerosols in these regions.

Our study indicates that the simulated AOT is sensitive to the RH resolution. Two questions raised here are whether the AOT continues to increase when the RH resolution is increased, and whether a 'best' resolution can be determined that represents

Change of AOT and aerosol DRE to RH

H. Bian et al.

Title Page

Abstract

Introduction

Conclusions

References

Tables

Figures

◀

▶

◀

▶

Back

Close

Full Screen / Esc

Printer-friendly Version

Interactive Discussion



a promise between accuracy and model efficiency. Instinctively, we think that such a resolution can be found because the sensitivity of the AOT will decline as the spatial (or temporal) heterogeneity of RH between grid boxes (or over an averaged period) weakens as the resolution increases. The resolution required for an adequate accuracy is likely depends on region. Our results indicate that the middle latitudes of both hemispheres tend to require a higher resolution than tropical regions in order to have the same AOT variation when RH resolution varies.

Our study indicates that the 24% diversity among the AOT annual global means (i.e. 0.11–0.14) from 20 different modules in an AeroCom AOT study (Kinne et al., 2006) could be easily induced by the varying model resolutions since the RH resolutions of the involved modules change about 186 times (i.e. from 1.1° (latitude) $\times 1.1^\circ$ (longitude) to $10^\circ \times 22.5^\circ$). Of course, the complexity of an aerosol physical and chemical system makes a conclusion more difficult. One way to improve the performance of a system is to better understand each process. The key conclusion of this paper is that increasing RH resolution increases the simulated AOT (and DRE). In other words, a high resolution model should have a larger, yet close to reality, AOT simulation than a low resolution model, and vice versa. If not (very likely due to the complexity of the system), then further investigation is required. In the AeroCom comparison, we need to bear this in mind.

The objective of this paper was to investigate the potential AOT and aerosol DRE bias resulting from the use of different model resolutions in model intercomparisons. The study of the three RH fields, representing current commonly used model resolutions, serves as a first step toward this goal. Nevertheless, the magnitude of the AOT variation associated with the RH resolution is subject to several limitations in the model's ability to resolve aerosol microphysical processes in the real atmosphere (Haywood et al., 1997, 1998; Ghan and Easter, 1998). Exploration of the activation of aerosol particles in cloudy regions is beyond the scope of this study.

The variation of AOT with RH field is a broad issue. In addition to MEE uncertainty (as well as AOT) due to the sub-grid RH variation as we discussed in this paper, the

Change of AOT and aerosol DRE to RH

H. Bian et al.

[Title Page](#)[Abstract](#)[Introduction](#)[Conclusions](#)[References](#)[Tables](#)[Figures](#)[I◀](#)[▶I](#)[◀](#)[▶](#)[Back](#)[Close](#)[Full Screen / Esc](#)[Printer-friendly Version](#)[Interactive Discussion](#)

Change of AOT and aerosol DRE to RH

H. Bian et al.

[Title Page](#)[Abstract](#)[Introduction](#)[Conclusions](#)[References](#)[Tables](#)[Figures](#)[I◀](#)[▶I](#)[◀](#)[▶](#)[Back](#)[Close](#)[Full Screen / Esc](#)[Printer-friendly Version](#)[Interactive Discussion](#)

aerosol MEE could also vary significantly even at a given RH. For example, measurements during recent field campaigns indicated that, compared to the value of dry ($\text{RH} \leq 40\%$) sulfate particles, the sulfate MEE at RH 85% was enhanced by about 3.5 times for ACEAsia, 3.0 for ICARTT, and 2.0 for INDOEX (Quinn et al., 2005). The value was 3.3 in our model. Part of the reason for such a large MEE uncertainty at RH 85% may be the different aerosol heritages in the different environments. Currently, most global/regional models parameterize aerosol size distribution and refractive index, which determine MEE through the Mie-theory, to be an empirical function of RH based on limited observations (Köpke et al., 1997; Chin et al., 2002). Clearly, this approach implies uncertainties in the growth calculation because

1. the fitting curve was frequently obtained from observational data that has a wide range;
2. the sampled observations may not fully represent the complexity of atmospheric processes due to different aerosol composition and the heritage of the particles (i.e. deliquescence and crystallization) (Jordanov and Zellner, 2006; Pant et al., 2006; Chan et al., 2006; Semeniuk et al., 2007).

References

- Bloom, S., da Silva, A., Dee, D., Bosilovich, M., Chern, J. D., et al.: Documentation and Validation of the Goddard Earth Observing System (GEOS) Data Assimilation System-Version 4, NASA/TM-2005-104606, 26, 2005.
- Chan, M. N., Lee, A. K. Y., and Chan, C. K.: Responses of ammonium sulfate particles coated with glutaric acid to cyclic changes in relative humidity: Hygroscopicity and Raman characterization, *Environ. Sci. Tech.*, 40(22), 6983–6989, 2006.
- Chin, M., Ginoux, P., Holben, B. N., Chou, M.-D., Kinne, S., and Weaver, C.: The GOCART model study of aerosol composition and radiative forcing, paper presented at 12th Symposium on Global Change and Climate Variations, Am. Meteorol. Soc., Albuquerque, New Mexico, USA, 2001.

Chin, M., Ginoux, P., Kinne, S., Torres, O., Holben, B. N., Duncan, B. N., et al.: Tropospheric aerosol optical thickness from the GOCART model and comparisons with satellite and sun photometer measurements, *J. Atmos. Sci.*, 59, 461–483, 2002.

Chin, M., Chu, A., Levy, R., Remer, L., Kaufman, Y., Holben, B., Eck, T., Ginoux, P., and Gao, Q.: Aerosol distribution in the Northern Hemisphere during ACE-Asia: results from global model, satellite observations, and sunphotometer measurements, *J. Geophys. Res.*, 109, D23S90, doi:10.1029/2004JD004829, 2004.

Chou, M.-D. and Suarez, M. J.: A solar radiation parameterization for atmospheric studies, Technical Report Series on Global Modeling and Data Assimilation, NASA Tech. Memo. 104606, 15, 40 pp., 1999.

Christopher, S. A. and Zhang, J.: Shortwave aerosol radiative forcing from MODIS and CERES observations over the oceans, *Geophys. Res. Lett.*, 29, 1859, doi:10.1029/2002GL014803, 2002.

Considine, D. B., Connell, P. S., Bergmann, D. J., Rotman, D. A., and Strahan, S. E.: Sensitivity of Global Modeling Initiative model predictions of Antarctic ozone recovery to input meteorological fields, *J. Geophys. Res.*, 109, D15301, doi:10.1029/2003JD004487, 2004.

Douglass, A. R., Connell, P. S., Stolarski, R. S., and Strahan, S. E.: Radicals and reservoirs in the GMI chemistry and transport model: comparison to measurements, *J. Geophys. Res.*, 109, D16302, doi:10.1029/2004JD004632, 2004.

Douglass, A. R., Stolarski, R. S., Strahan, S. E., and Polansky, B. C.: Sensitivity of Arctic ozone loss to polar stratospheric cloud volume and chlorine and bromine loading in a chemistry and transport model, *Geophys. Res. Lett.*, 33, L17809, doi:10.1029/2006GL026492, 2006.

Patadia, F., Gupta, P., and Christopher, S. A.: First estimates of global shortwave aerosol direct radiative effect over land using merged CERES, MODIS and MISR data, *Geophys. Res. Lett.*, 35, L04810, doi:10.1029/2007GL032314, 2008.

Ghan, S. and Easter, R. C.: Comments on “A limited-area-model case study of the effects of sub-grid scale variation in relative humidity and cloud upon the direct radiative forcing of sulfate aerosol”, *Geophys. Res. Lett.*, 25(7), 1039–1040, 1998.

Ginoux, P., Chin, M., Tegen, I., Prospero, J. M., Holben, B., Dubovik, O., and Lin, S.-J.: Sources and distributions of dust aerosols simulated with the GOCART model, *J. Geophys. Res.*, 106(D17), 20 255–20 273, 2001.

Gong, S., Barrie, L. A., and Blanchet, J.-P.: Modeling sea salt aerosols in the atmosphere, 1: Model development, *J. Geophys. Res.*, 102, 3805–1818, 1997.

Change of AOT and aerosol DRE to RH

H. Bian et al.

Title Page

Abstract

Introduction

Conclusions

References

Tables

Figures

◀

▶

◀

▶

Back

Close

Full Screen / Esc

Printer-friendly Version

Interactive Discussion



Change of AOT and aerosol DRE to RH

H. Bian et al.

Title Page

Abstract

Introduction

Conclusions

References

Tables

Figures

◀

▶

◀

▶

Back

Close

Full Screen / Esc

Printer-friendly Version

Interactive Discussion



Haywood, J. M., Ramaswamy, V., and Donner, L. J.: A limited-area-model case study of the effects of sub-grid scale variation in relative humidity and cloud upon the direct radiative forcing of sulfate aerosol, *Geophys. Res. Lett.*, 24(2), 143–146, 1997.

Haywood, J. M., Ramaswamy, V., and Donner, L. J., Reply, *Geophys. Res. Lett.*, 25(7), 1041, 1998.

Intergovernmental Panel on Climate Change (IPCC): Climate Change 2001: synthesis Report, Third Assessment Report of the Intergovernmental Panel on Climate Change, Cambridge University Press, New York, USA, 2001.

Jordanov, N. and Zekker, R.: Investigations of the hygroscopic properties of ammonium sulfate and mixed ammonium sulfate and glutaric acid micro droplets by means of optical levitation and Raman spectroscopy, *Phys. Chem. Chem. Phys.*, 8(23), 2759–2764, 2006.

Kinne, S., Schulz, M., Textor, C., Guibert, S., Balkanski, Y., et al.: An AeroCom initial assessment: optical properties in aerosol component modules of global models, *Atmos. Chem. Phys.*, 6, 1815–1834, 2006,

<http://www.atmos-chem-phys.net/6/1815/2006/>.

Liu, X., Penner, J. E., Das, B., et al.: Uncertainties in global aerosol simulations: assessment using three meteorological datasets, *J. Geophys. Res.*, 112, D11212, doi:10.1029/2006JD008216, 2007.

Malm, W. C., Day, D. E., Kreidenweis, S. M., Collett, J. L., Carrico, C., McMeeking, G., and Lee, T.: Hygroscopic properties of an organic-laden aerosol, *Atmos. Environ.*, 39(27), 4969–4982, 2005.

Monahan, E. C., Spiel, D. E., and Davidson, K. L.: A model of marine aerosol generation via whitecaps and wave disruption, *Oceanic Whitecaps*, edited by: Monahan, E. C. and MacNiocaill, G., D. Reidel Publishing, Dordrecht, The Netherlands, 167–174, 1986.

Pahlow, M., Feingold, G., Jefferson, A., Andrews, E., Ogren, J. A., Wang, J., Lee, Y. N., Ferrare, R. A., and Turner, D. D.: Comparison between lidar and nephelometer measurements of aerosol hygroscopicity at the Southern Great Plains Atmospheric Radiation Measurement site, *J. Geophys. Res.*, 111(D5), D05S15, doi:10.1029/2004JD005646, 2006.

Pant, A., Parsons, M. T., and Bertram, A. K.: Crystallization of aqueous ammonium sulfate particles internally mixed with soot and kaolinite: crystallization relative humidities and nucleation rates, *J. Phys. Chem. A*, 110(28), 8701–8709, 2005.

Quinn, P. K., Bates, T. S., Baynard, T., Clarke, A. D., Onasch, T. B., Wang, W., Rood, M. J., Andrews, E., Allan, J., Carrico, C. M., Coffiman, D., and Worsnop, D.: Impact of particulate

Change of AOT and aerosol DRE to RH

H. Bian et al.

Title Page

Abstract

Introduction

Conclusions

References

Tables

Figures

◀

▶

◀

▶

Back

Close

Full Screen / Esc

Printer-friendly Version

Interactive Discussion



- organic matter on the relative humidity dependence of light scattering: a simplified parameterization, *Geophys. Res. Lett.*, 32, L22809, doi:10.1029/2005GL024322, 2005.
- Semeniuk, T. A., Wise, M. E., Martin, S. T., Russell, M., and Buseck, P. R.: Hygroscopic behavior of aerosol particles from biomass fires using environmental transmission electron microscopy, *J. Atmos. Chem.*, 56(3), 259–273, 2007.
- Schulz, M., Textor, C., Kinne, S., Balkanski, Y., Bauer, S., et al.: Radiative forcing by aerosols as derived from the AeroCom present-day and pre-industrial simulations, *Atmos. Chem. Phys.*, 6, 5225–5246, 2006, <http://www.atmos-chem-phys.net/6/5225/2006/>.
- Strahan, S.E. and Douglass, A. R.: Evaluating the credibility of transport processes in simulations of ozone recovery using the Global Modeling Initiative three-dimensional model, *J. Geophys. Res.*, 109, D05110, doi:10.1029/2003JD004238, 2004.
- Strahan, S. E. and Polansky, B. C.: Meteorological implementation issues in chemistry and transport models, *Atmos. Chem. Phys.*, 6, 2895–2910, 2006, <http://www.atmos-chem-phys.net/6/2895/2006/>.
- Strahan, S. E., Duncan, B. N., and Hoor, P.: Observationally derived transport diagnostics for the lowermost stratosphere and their application to the GMI chemistry and transport model, *Atmos. Chem. Phys.*, 7, 2435–2445, 2007, <http://www.atmos-chem-phys.net/7/2435/2007/>.
- Textor, C., Schulz, M., Guibert, S., Kinne, S., Balkanski, Y., et al.: Analysis and quantification of the diversities of aerosol life cycles within AeroCom, *Atmos. Chem. Phys.*, 6, 1777–1813, 2006, <http://www.atmos-chem-phys.net/6/1777/2006/>.
- Weaver, C. J., Ginoux, P., Hsu, N. C., Chou, M.-D., and Joiner, J.: Radiative Forcing of Saharan Dust: GOCART model simulations Compared with ERBE data, *J. Atmos. Sci.*, 59(3), 736–747, 2002.
- Yoon, S. C. and Kim, J.: Influences of relative humidity on aerosol optical properties and aerosol radiative forcing during ACE-Asia, *Atmos. Environ.*, 40(23), 4328–4338, 2006.
- Yu, H., Kaufman, Y. J., Chin, M., Feingold, G., Remer, L. A., et al.: A review of measurement-based assessments of the aerosol direct radiative effect and forcing, *Atmos. Chem. Phys.*, 6, 613–666, 2006, <http://www.atmos-chem-phys.net/6/613/2006/>.
- Zhang, J., Christopher, S. A., Remer, L. A., and Kaufman, Y. J.: Shortwave aerosol radiative

forcing over cloud-free oceans from Terra, 2: seasonal and global distribution, J. Geophys. Res., 110, D10S24, doi:10.1029/2004JD005009, 2005.

ACPD

8, 13233–13263, 2008

Change of AOT and aerosol DRE to RH

H. Bian et al.

Title Page

Abstract

Introduction

Conclusions

References

Tables

Figures

◀

▶

◀

▶

Back

Close

Full Screen / Esc

Printer-friendly Version

Interactive Discussion



Change of AOT and aerosol DRE to RH

H. Bian et al.

Table 1. Spatial and temporal resolutions of RH used in the three experiments^a.

experiments	spatial resolution ^b (latitude×longitude)	averaged over (h)
BASE	2°×2.5° ^c	3
CTRH	1°×1.25°	3
CTRTR	2°×2.5°	6

^a All experiments use GMI aerosol mass with spatial resolution 2°×2.5°.

^b All experiments have 42 vertical layers to top lit at 0.01 mb.

^c RH averaged from 1°×1.25°.

[Title Page](#)[Abstract](#)[Introduction](#)[Conclusions](#)[References](#)[Tables](#)[Figures](#)[◀](#)[▶](#)[◀](#)[▶](#)[Back](#)[Close](#)[Full Screen / Esc](#)[Printer-friendly Version](#)[Interactive Discussion](#)

Change of AOT and aerosol DRE to RH

H. Bian et al.

Table 2. The aerosol TOA DREs of the three experiments and the percentage changes of the aerosol DREs between the controlled and base cases.

		Ocean			Land			Global		
		BASE	CTRH	CTRT	BASE	CTRH	CTRT	BASE	CTRH	CTRT
clear sky	DRE (W/m ²)	-4.4	-4.8	-4.2	-8.4	-9.1	-8.3	-5.6	-6.1	-5.4
	dDRE* (%)		8.9	3.5		8.0	2.1		8.4	2.9
whole sky	DRE (W/m ²)	-3.3	-3.6	-3.2	-6.9	-7.4	-6.8	-4.4	-4.8	-4.3
	dDRE (%)		9.3	3.1		7.7	1.9		8.5	2.6

* $dDRE(CTRH) = [AOT(CTRH) - AOT(BASE)] / AOT(BASE)$
 $dDRE(CTRT) = [AOT(BASE) - AOT(CTRT)] / AOT(CTRT)$

[Title Page](#)
[Abstract](#)
[Introduction](#)
[Conclusions](#)
[References](#)
[Tables](#)
[Figures](#)
[Back](#)
[Close](#)
[Full Screen / Esc](#)
[Printer-friendly Version](#)
[Interactive Discussion](#)


Change of AOT and aerosol DRE to RH

H. Bian et al.

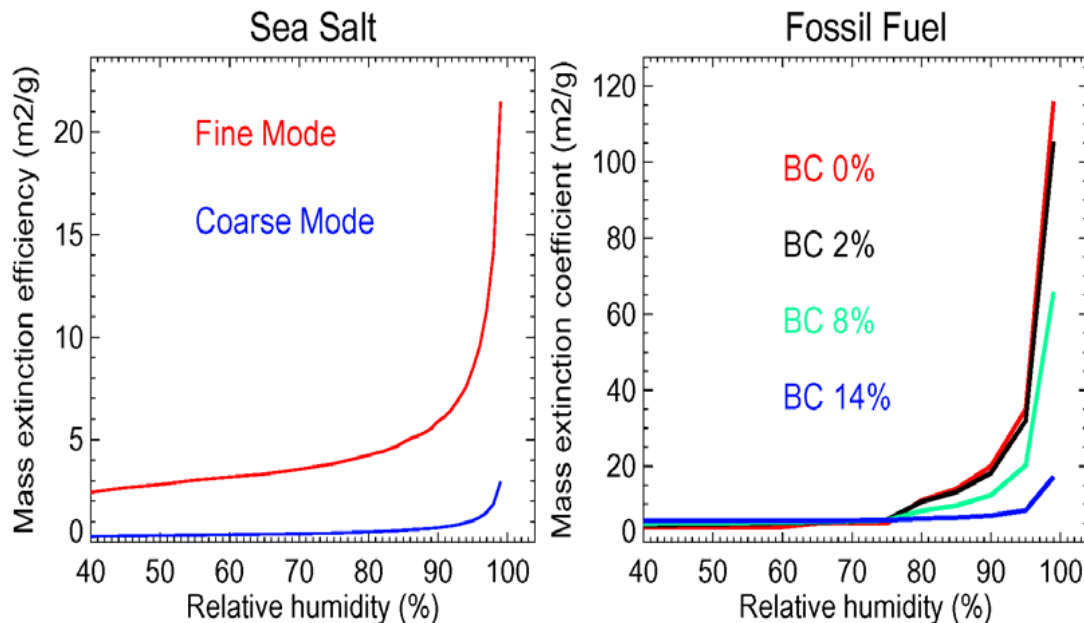


Fig. 1. Mass extinction efficiencies (at $\lambda=550$ nm) of sea salt particles (left) and fossil fuel particles (right) as a function of relative humidity. Two color lines in the left are corresponding to fine and coarse modes of sea salt particles. Fossil fuel aerosol contains internal mixed sulfate, black carbon, and organic carbon. Four color lines in the right are associated with four different aerosol compositions indicated by different weighted BC. MEEs are calculated by Mie-theory with the basic information of aerosol size distribution and refractive index.

[Title Page](#)[Abstract](#)[Introduction](#)[Conclusions](#)[References](#)[Tables](#)[Figures](#)[I◀](#)[▶I](#)[◀](#)[▶](#)[Back](#)[Close](#)[Full Screen / Esc](#)[Printer-friendly Version](#)[Interactive Discussion](#)

Change of AOT and
aerosol DRE to RH

H. Bian et al.

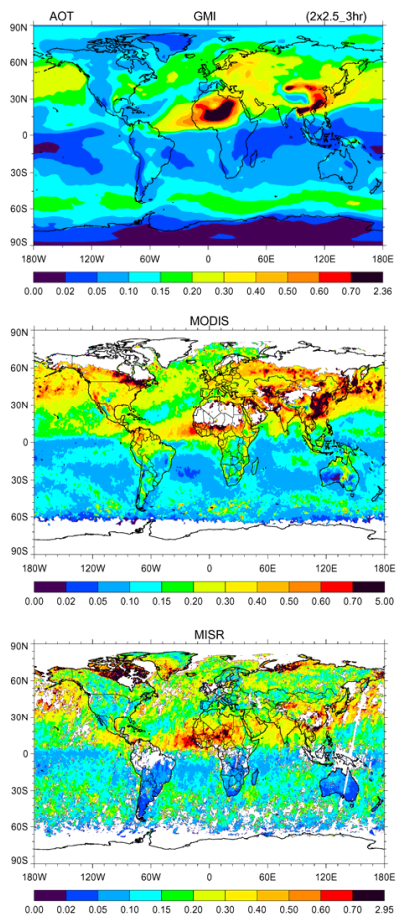


Fig. 2. Aerosol Optical Thickness (AOT) at 550 nm in April 2001 from GMI base case simulation (upper panel) and satellite measurements of MODIS (middle panel) and MISR (lower-panel).

[Title Page](#)[Abstract](#)[Introduction](#)[Conclusions](#)[References](#)[Tables](#)[Figures](#)[◀](#)[▶](#)[◀](#)[▶](#)[Back](#)[Close](#)[Full Screen / Esc](#)[Printer-friendly Version](#)[Interactive Discussion](#)

Change of AOT and aerosol DRE to RH

H. Bian et al.

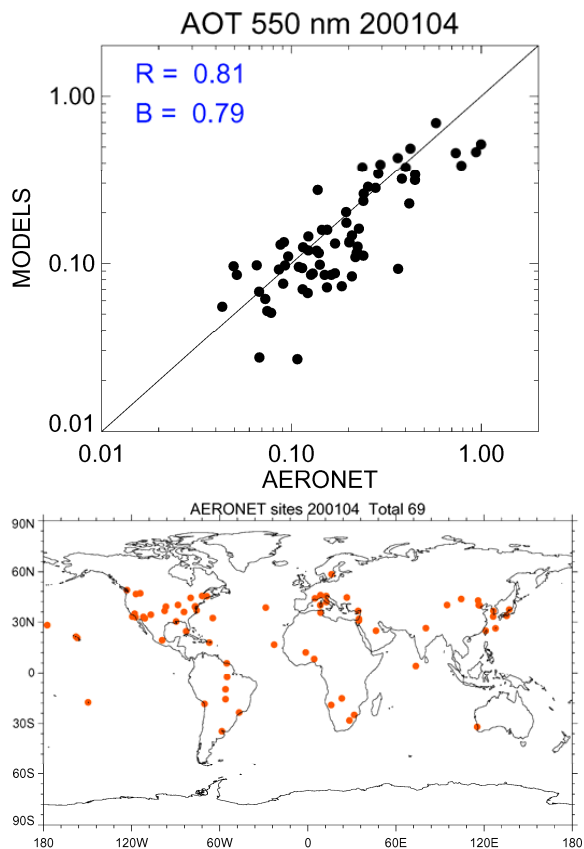


Fig. 3. Comparison of AOT (550 nm) in April 2001 between GMI simulation and AERONET measurement (upper panel) over AERONET sites (lower panel). The R and B are the correlation and relative bias between model and measurement respectively.

[Title Page](#)[Abstract](#)[Introduction](#)[Conclusions](#)[References](#)[Tables](#)[Figures](#)[◀](#)[▶](#)[◀](#)[▶](#)[Back](#)[Close](#)[Full Screen / Esc](#)[Printer-friendly Version](#)[Interactive Discussion](#)

Change of AOT and
aerosol DRE to RH

H. Bian et al.

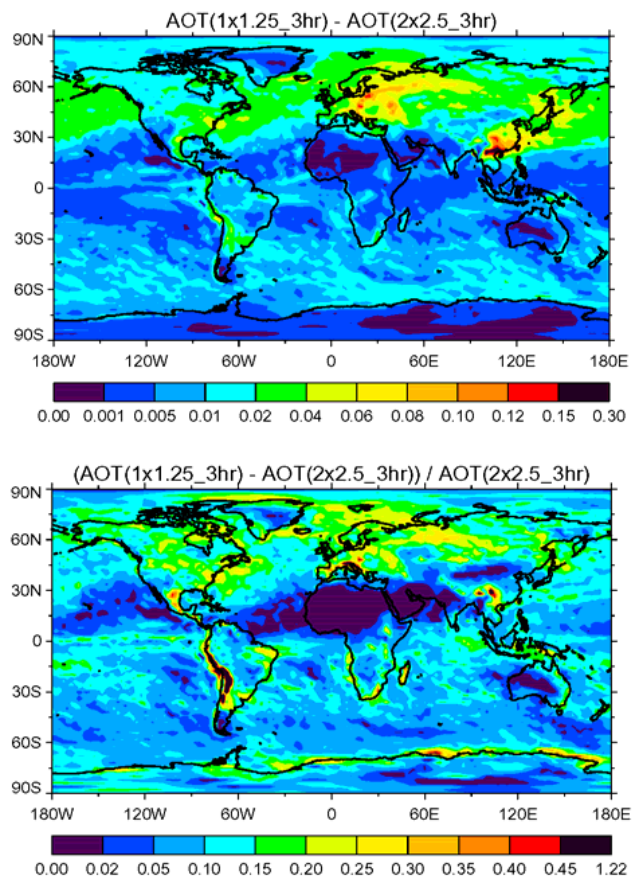


Fig. 4. Absolute (upper-panel) and relative (lower-panel) monthly mean AOT differences in April 2001 when use RH horizontal resolution of $1^\circ(\text{latitude}) \times 1.25^\circ(\text{longitude})$ vs. $2^\circ \times 2.5^\circ$.

[Title Page](#)[Abstract](#)[Introduction](#)[Conclusions](#)[References](#)[Tables](#)[Figures](#)[I◀](#)[▶I](#)[◀](#)[▶](#)[Back](#)[Close](#)[Full Screen / Esc](#)[Printer-friendly Version](#)[Interactive Discussion](#)

Change of AOT and aerosol DRE to RH

H. Bian et al.

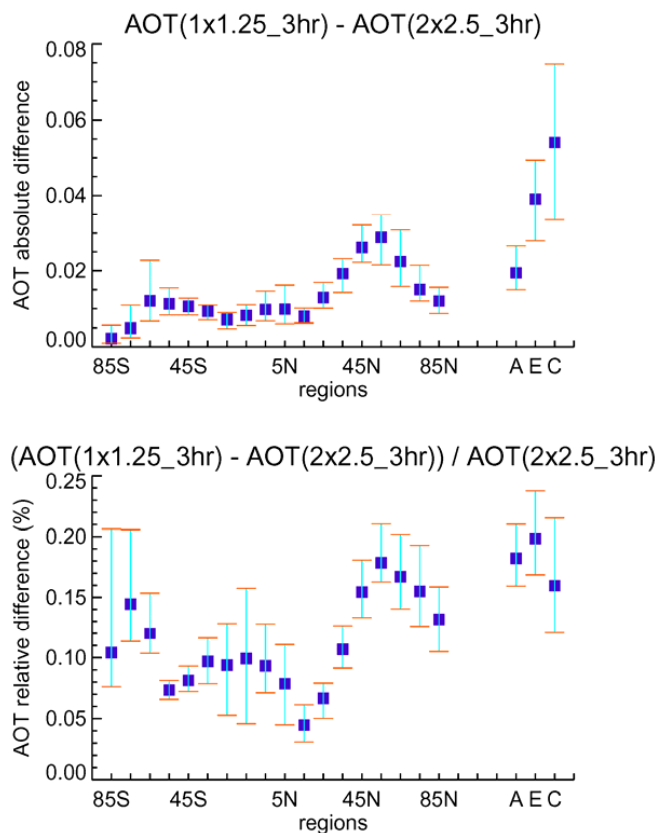


Fig. 5. Zonal mean AOT absolute (upper panel) and relative (lower panel) changes in every 10° latitudes caused by the change of RH horizontal resolutions. Blue squares are annual averaged values. The vertical bars represent the seasonal variations. In the most right are regional data for eastern America (A), Western Europe (E), and eastern China (C).

[Title Page](#)[Abstract](#)[Introduction](#)[Conclusions](#)[References](#)[Tables](#)[Figures](#)[◀](#)[▶](#)[◀](#)[▶](#)[Back](#)[Close](#)[Full Screen / Esc](#)[Printer-friendly Version](#)[Interactive Discussion](#)

Change of AOT and aerosol DRE to RH

H. Bian et al.

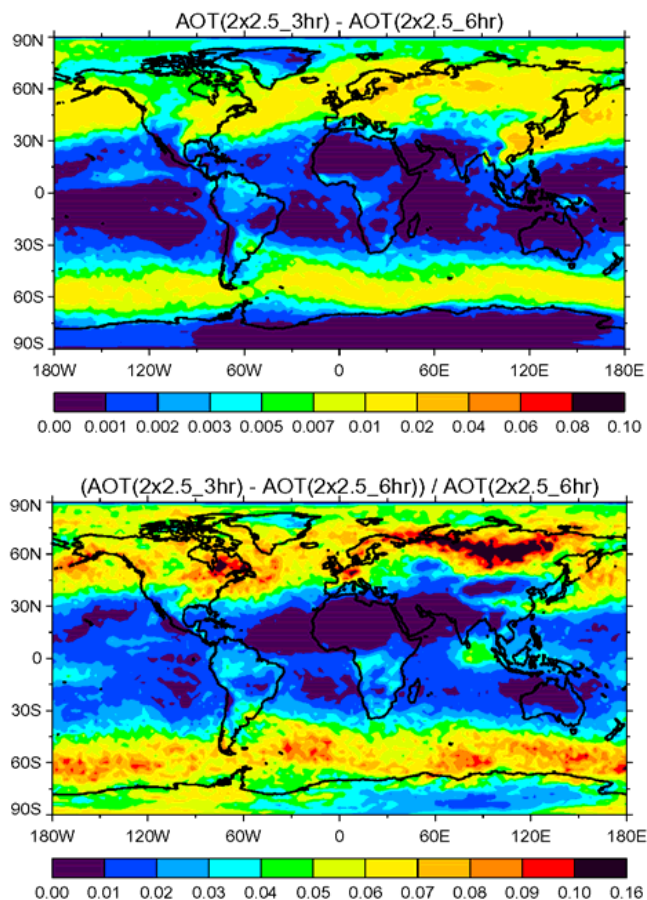


Fig. 6. Similar to Fig. 4, but with RH averaged over 3-h intervals vs. 6-h intervals (note scale difference with Fig. 4).

[Title Page](#)[Abstract](#)[Introduction](#)[Conclusions](#)[References](#)[Tables](#)[Figures](#)[I◀](#)[▶I](#)[◀](#)[▶](#)[Back](#)[Close](#)[Full Screen / Esc](#)[Printer-friendly Version](#)[Interactive Discussion](#)

Change of AOT and aerosol DRE to RH

H. Bian et al.

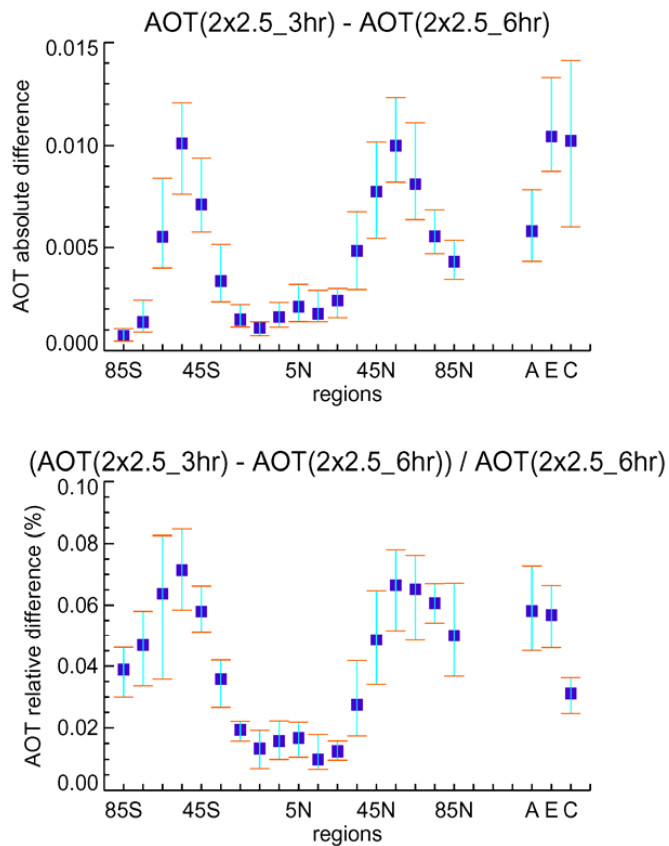


Fig. 7. Similar to Fig. 5, but for the change of RH temporal resolutions.

[Title Page](#)[Abstract](#)[Introduction](#)[Conclusions](#)[References](#)[Tables](#)[Figures](#)[I◀](#)[▶I](#)[◀](#)[▶](#)[Back](#)[Close](#)[Full Screen / Esc](#)[Printer-friendly Version](#)[Interactive Discussion](#)

Change of AOT and
aerosol DRE to RH

H. Bian et al.

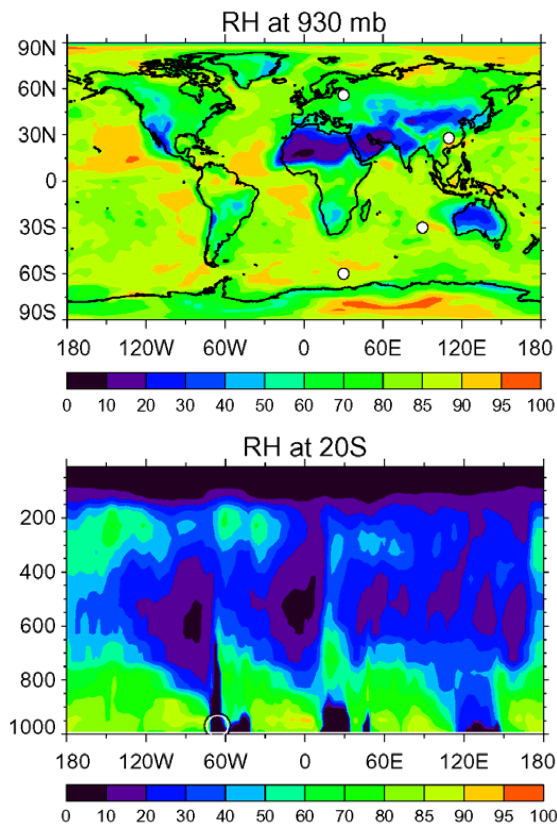


Fig. 8. Global RH field for April 2001 at the vertical layer of 930 mb (upper panel). The detail RH change over four locations (white circles) will show in Fig. 9. The lower panel shows vertical-longitude RH (2×2.5 .3h) distribution at latitude 20°S for April 2001. Andes Mountain is located around longitude 60° – 70° W as indicated by an open black circle.

[Title Page](#)[Abstract](#)[Introduction](#)[Conclusions](#)[References](#)[Tables](#)[Figures](#)[◀](#)[▶](#)[◀](#)[▶](#)[Back](#)[Close](#)[Full Screen / Esc](#)[Printer-friendly Version](#)[Interactive Discussion](#)

Change of AOT and aerosol DRE to RH

H. Bian et al.

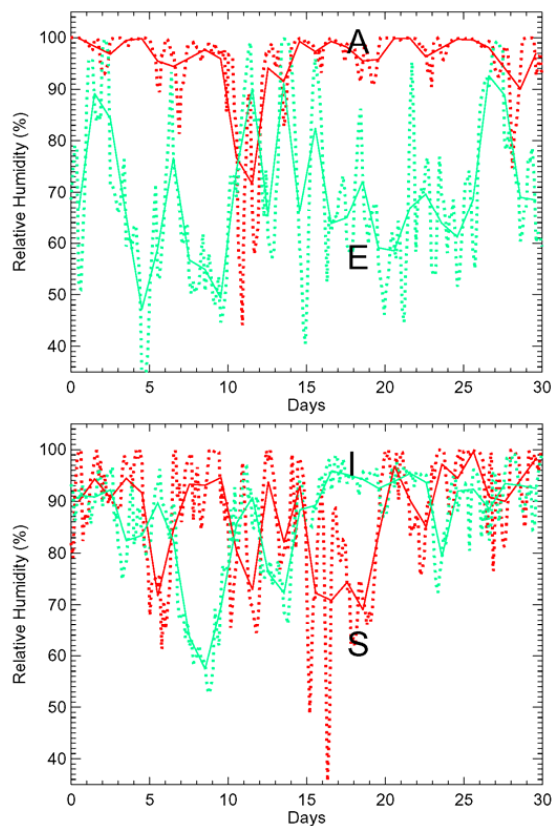


Fig. 9. RH at two land sites (upper panel) and two ocean sites (lower panel). The locations of the four sites (A (110° E, 28° N); E (30° E, 56° N); I (90° E, 30° S); and S (30° E, 60° S)) are shown in Fig. 8 (white circles). The solid lines represent daily mean and dot lines are for 3-h average.

[Title Page](#)[Abstract](#)[Introduction](#)[Conclusions](#)[References](#)[Tables](#)[Figures](#)[I◀](#)[▶I](#)[◀](#)[▶](#)[Back](#)[Close](#)[Full Screen / Esc](#)[Printer-friendly Version](#)[Interactive Discussion](#)